1-1-2001

Scanner Parameter Estimation Using Bilevel Scans of Star Charts

Elisa H. Barney Smith
Boise State University

Scanner Parameter Estimation Using Bilevel Scans of Star Charts

Elisa H. Barney Smith

Electrical and Computer Engineering Department

Boise State University, Boise, Idaho 83725

EBarneySmith@boisestate.edu

Abstract

Scanning a high contrast image in bilevel mode results in image degradation. This is caused by two primary effects: blurring and thresholding. This paper expands on a method of estimating a joint distortion parameter, called the edge spread, from a star sector test chart in order to calculate the values of the point spread function width and binarization threshold. This theory is also described for variations in the source pattern which can represent degradations caused by repetition of the bilevel process as would be seen in printing then scanning, or in repeated photocopying. Estimation results are shown for the basic and extended cases.

1. Introduction

In a bilevel image, only the position of the edge, not the greylevel profile, is visible. Thus, the methods used to estimate the point spread function (PSF) width from a grey-level scan will not transfer to a bilevel scan. Also, the threshold level used to convert a grey-level scan into a bilevel scan becomes an additional parameter that needs to be estimated.

This paper describes a method of estimating both the PSF width and the threshold level from bilevel scans of high contrast images. Knowledge of the PSF and binarization threshold can improve OCR by facilitating the creation of training sets matched to the expected nature and degree of image degradation in the target document [2, 5]. This paper starts with a review of the estimation of the edge spread, δ_c, from a star sector test target. The parameter δ_c is a function of both PSF width and binarization threshold.

The main portion of this paper describes a method of estimating PSF width, w, and binarization threshold, Θ, parameters individually. This theory is then extended to consider defects present when an image is passed through multiple bilevel systems, as in repeated photocopying. The paper ends with examples of estimation results.

2. Estimating the Edge Displacement Parameter for a Scanner

The effect of bilevel scanning on a printed line (i.e.,

changes in line width) was quantified in a single parameter, δ_c, in [3, 4]. This parameter is a composite of the two parameters that have the greatest effect on scanning distortions: the diameter of the point spread function, w, and the intensity threshold, Θ [5].

The edge spread is the change in the edge location from its original (paper) position relative to the scanning grid to its position in the digitized image. The edge spread, δ_c, is measured from the change in spacing between pairs of sector edges in a star target (Figure 1). Several edges provide the average edge displacement, which can be calculated to sub-pixel accuracy reducing spatial quantization noise. Measurements of the change in edge location in areas both where there is and where there is no interference will allow the thresholding effects and the PSF size effects to be separated. The edges are also distributed in phase relative to the sampling grid, which reduces the random-phase effects discussed in [7].

Star targets were also suggested for defect model calibration in [1]. A star chart is assumed to have black and white sectors of equal width, τ, directly proportional to the radius (traverse a circle concentric with the center of the chart). The white sectors have a value of 0 and the black sectors have a value of 1. Alternate assumptions will be discussed after the theory is fully developed under these basic assumptions.

In Figure 2a, an edge spread function (ESF) is shown for two PSF widths, w. If the equation representing the ESF for a unit width parameter is ESF(x), then the new edge location for a threshold of Θ would occur at $x=-\delta_c$ or

$$\Theta = \text{ESF}(-\delta_c). \tag{1}$$

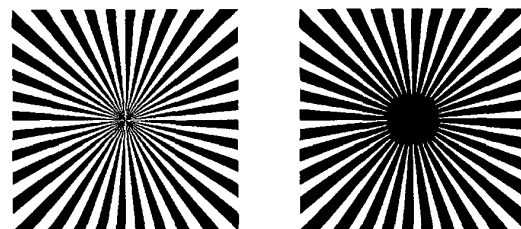If the width of the PSF is parameterized by w, then the

Figure 1: A star sector test target with 36 black-and-white sectors of equal width before (left) and after (right) bilevel scanning.
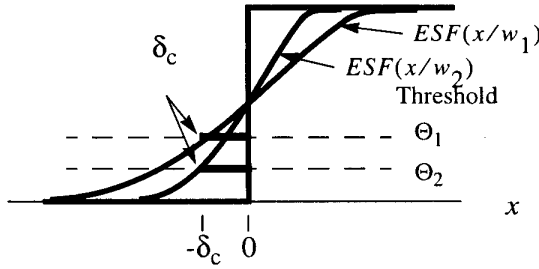
Figure 2: Edge after blurring with a generic PSF of two widths, w. Two thresholds are shown that produce the same edge shift δ_c.
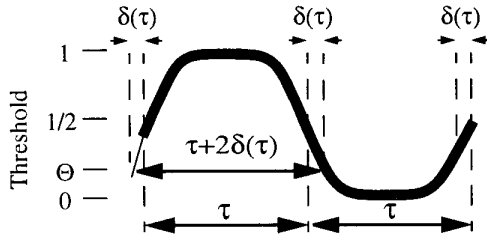

Figure 3: Blurring affects the fraction of one period of a blurred pulse train that will exceed a threshold Θ.

general form would be

$$\Theta = \text{ESF}(-\delta_c / w) , \qquad (2)$$

so

$$\delta_c = -w \, \text{ESF}^{-1}(\Theta) . \qquad (3)$$

There are multiple values of w and Θ that result in the same value of δ_c, and thus produce the same distortion on an isolated edge.

The parameter δ_c can be measured from a star chart. A star chart can be decomposed into a series of pulse trains with black-and-white segments of equal length, τ, proportional to the radii of circular paths around the star center. Figure 3 shows one full period of a blurred pulse train. The fraction of a pulse train located above the threshold will be

$$fr(\tau) = \frac{\tau + 2\delta(\tau)}{2\tau} . \qquad (4)$$

The average displacement of the edges after blurring and thresholding is calculated by measuring the fraction of black pixels along each circular trajectory, $fr(\tau)$, from the scanned star target.

There will be no interference between edges separated by $\tau > w$ (Figure 4) if the support of the PSF is finite. In this case the edge displacement will be constant

$$\delta(\tau) = \left(fr(\tau) - \frac{1}{2}\right)\tau = \delta_c . \qquad (5)$$

Because w and Θ are not known, δ_c is measured by looking for the values of τ where $\delta(\tau)$ is constant.

If the support of the PSF is infinite, there will always be interference between multiple edges, so $\delta(\tau)$ will not be
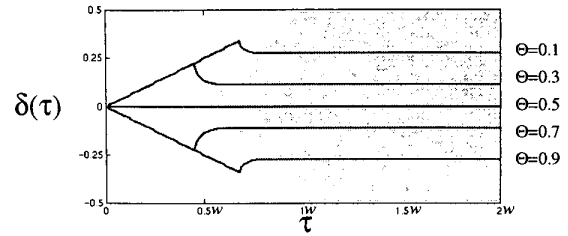

Figure 4: Edge spread $\delta(\tau)$ vs. τ for a triangular PSF of unit width at several thresholds. The curves are horizontal when there is no interference between edges (shaded region).

constant. At some large value of τ, the amount of interference will be small, the $\delta(\tau)$ curve will level out, and δ_c can be measured. For PSF with infinite support, such as Gaussian or Cauchy, the entire star will be in the interference regions. The amount of interference is small at large τ values and the $\delta(\tau)$ function will, in the limit, approach the δ_c value. In practice, $\delta(\tau)$ will approach δ_c rapidly, allowing δ_c to be measured.

3. Using Sector Merge Width to Estimate PSF Width & Threshold

The measurement of the edge shift δ_c was based on the use of isolated edges. As τ decreases, it is certain that the effects of blurring on neighboring edges such as described in [6] will be a factor. The manner in which the blurring of neighboring edges interact provides information that can be used to get individual values for the PSF width and binarization threshold parameters.

When edges are closer together than the support of the PSF, the amplitude of the pulse train after blurring reaches its extreme values between 0 and 1 exclusively. If the threshold is above (below) the maximum (minimum) amplitude of the blurred pulse train, the star chart will be all black (white). The edge spread distance will be either $\tau/2$ or $-\tau/2$, which is the minimum edge displacement needed to merge two adjacent sectors of the same color.

For a given threshold, there are several values of τ where the sectors are merged. The largest value of τ at which $|\delta(\tau)| = \tau/2$ occurs when the threshold reaches exactly the blurred pulse train amplitude and is called the *sector merge width*, τ_1 (Figure 5). Merging can be seen where the white wedges vanish into the center black region (Figure 1). The parameters τ_1 and δ_c are each functions of both PSF width and threshold. Measurements of δ_c and τ_1, together with the two equations relating each of them to w and Θ, lead to estimates for both PSF width and threshold.

The thresholds corresponding to the maximum and minimum amplitudes of the blurred pulse train, Θ_{MAX} and Θ_{MIN}, are functions of τ_1/w. Combining these with the δ_c

1165
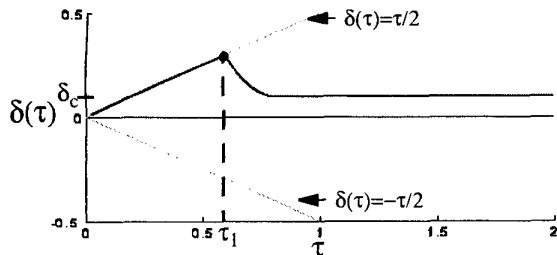
Figure 5: Representative $\delta(\tau)$ **curve.** $\delta(\tau) = \tau/2$ **for all** $\tau<\tau_1$.

formula in Equation 3, the corresponding equations are

$$\delta_{c\ HIGH}/w = -ESF^{-1}(\Theta_{MAX}) \qquad (6)$$

and

$$\delta_{c\ LOW}/w = -ESF^{-1}(\Theta_{MIN}) . \qquad (7)$$

The Θ value is replaced by its relation to τ_1 and w and δ_c is related to τ_1 by the *asymptotic edge displacement* (AED) functions

$$\delta_c/w = -ESF^{-1}(\Theta_{function}(\tau_1/w)) . \qquad (8)$$

The AED functions have an unknown scaling factor of w on both variables and need only be calculated for one PSF width; the others can be found by scaling. The AED functions for the triangle pulse and for the Gaussian PSF are shown in Figures 6a & b, respectively. Note the difference between PSFs with a finite and infinite support. The scale, w, which makes the observed (τ_1, δ_c) point lie on the curve, is the correct value. Once the PSF width is found, the intensity threshold, Θ, is determined using Equation 2. Note that if $\Theta=0.5$, τ_1 is zero, so is δ_c for all PSF widths w, therefore this method does not work.

For a general PSF form, the estimation procedure will be:

1) Measure $\delta(\tau)$ by measuring the fraction for all τ and converting with Equation 5.
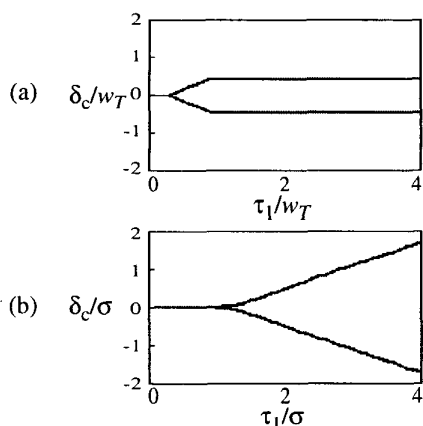
Figure 6: Asymptotic edge displacement (AED) for unit width (a) triangular pulse and (b) Gaussian PSF.

2) Estimate δ_c from the $\delta(\tau)$ curve in the horizontal region (large values of τ).

3) Measure τ_1 from the maximum τ value for which $|\delta(\tau)|= \tau/2$.

4) Calculate the relation between max/min threshold and edge separation τ for a unit width PSF.

5) Translate this to AED functions (Figure 6) relating sector merge width, τ_1, and edge displacement, δ_c using Equations 6 & 7. Scale the AED functions by the PSF parameter, w, until the measured data point lies on the curve. This scale factor is the value of the PSF width parameter, w.

6) Use the estimate of w, together with the measurement of δ_c, to get an estimate of the binarization threshold Θ, using Equation 2.

4. The Effects of Varying the Test Pattern Sector Widths

The derivations for estimation of scanner system parameters from sector merge widths specified using a star chart with black and white sectors of equal widths (Figure 7a). If the sector edge is shifted parallel to the ideal edge position (Figure 7b), the sector widths are not equal. This deformation will cause measurements for the estimation method to be different than those predicted by the theory, resulting in estimation errors. This section discusses how to adjust the theory if this criteria is relaxed.

The parallel edge deformation may occur in the printed chart through the same process of blurring and thresholding that is being modeled for the scanner. Printing can often be considered a bilevel process similar to scanning, but with a different (higher) resolution. The edge shift Δ could be a spread equivalent to δ_c that occurs during the printing process, or it could be due to a finite size border line. Thus, this discussion leads to the degradations caused by repetition of the bilevel process as would be seen in printing then scanning, or in photocopying.

With this new chart description, the black and white sector widths, τ_b and τ_w, will no longer be equal. The sector widths will be related by

(a)   (b)
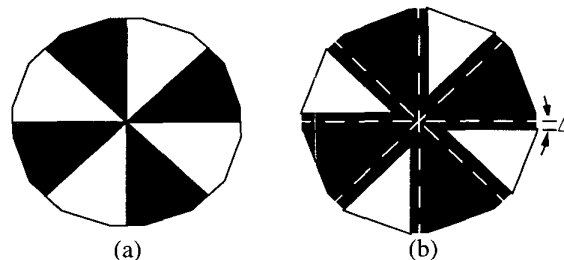
Figure 7: (a) Ideal star with equal sized sectors. (b) Star with parallel edge deformation.

1166

$$\tau_b = \tau_w + \Delta \qquad (9)$$

and

$$\tau = \frac{\tau_b + \tau_w}{2} \qquad (10)$$

in which case

$$\tau = \frac{2\tau_b - \Delta}{2} . \qquad (11)$$

Unequal sector widths affect the fraction of the pulse train that is black before and after blurring and thresholding. The fraction of a skewed pulse train that is above the threshold in regions where there is no aliasing will be

$$fr_{skewed}(\tau) = \frac{\tau_b + 2\delta(\tau)}{\tau_b + \tau_w} \qquad (12)$$

Combining equations 10, 11 and 12 will result in

$$\delta(\tau) = \tau \left[fr_{skewed}(\tau) - \frac{1}{2} \right] - \frac{\Delta}{4} . \qquad (13)$$

This difference in $\delta(\tau)$ produces a vertical shift in the $\delta(\tau)$ curve relative to a star with no parallel edge deformation. Near the center of the star where $\tau < |2\Delta|$, the neighboring edges will meet and the center of the star will become either all white or all black. Thresholds for which the center of the star was expected to be partially or totally white will often still result in a black center (or vice versa). This can not be corrected algebraically, and measurements of the sector merge width, τ_1, may not be accurate. This will affect the estimation that uses this measurement.

5. Results

Experiments were conducted to estimate the PSF width and the binarization thresholds using the sector merge distance. They were conducted on two scanners, a 600 dpi HP and a 300 dpi Apple, at 17 thresholds. The experiments were calibrated using estimates from grey scale scans. To estimate the PSF width and binarization threshold the functional form of the PSF must be assumed. Five PSF forms (square pulse, triangular pulse, raised cosine, Gaussian and Cauchy) were used.

In Figure 8, the estimated reflectance (1-Θ) is compared to the reflectance threshold at which the binary star was created. Table 1 shows the mean and standard deviation of the estimated width parameters across the multiple thresholds and the benchmark width parameters estimated using grey-scale knife edge in the horizontal and vertical directions for comparison. A range of true PSF widths are shown, as the PSF was found to be non-isotropic.

The discrepancies between the ideal star chart and the physical star chart play a large part in estimation inconsistencies. The stars on the Kodak test chart have white bands to provide visual clues of sector frequency. These bands interfere with the estimation by obscuring τ_1 estimates that fall in the bands and affect $fr(\tau)$ estimates for τ where the bands are within the support of the PSF. The value of τ_1 was estimated by extrapolating the $\delta(\tau)$ curve into the white bands on the Kodak chart. That star also does not show its center, so for thresholds near 0.5 the estimates are not available.

Another star chart without white bands, T2, was also used. This target had unequal sector widths produced by a parallel edge shift distortion. The amount of parallel edge deformation in the T2 target was estimated to be $\Delta \approx 0.5$. The edge displacement, $\delta(\tau)$, for the T2 chart scanned on the HP scanner was adjusted by the correction factors described in Section 4, and the adjusted (τ_1, δ_c) pairs were used to estimate the (w, Θ). This adjustment increased δ_c by $\Delta/4$. This correction leads to the estimates for PSF width and binarization threshold listed in Table 2. The number of invalid points was reduced and the estimates were slightly improved. However, correction is not possible near the center of the star where the sectors have merged.

These results show the mean width estimate is either between the width estimates from the grey-scale experiments, or within one standard deviation of these values. There is high correlation between the estimated reflectance and the reflectance corresponding to the level at which the bilevel star image was created. Some mismatch between the estimated and expected thresholds is associated with the need to scale the threshold estimates to compensate for
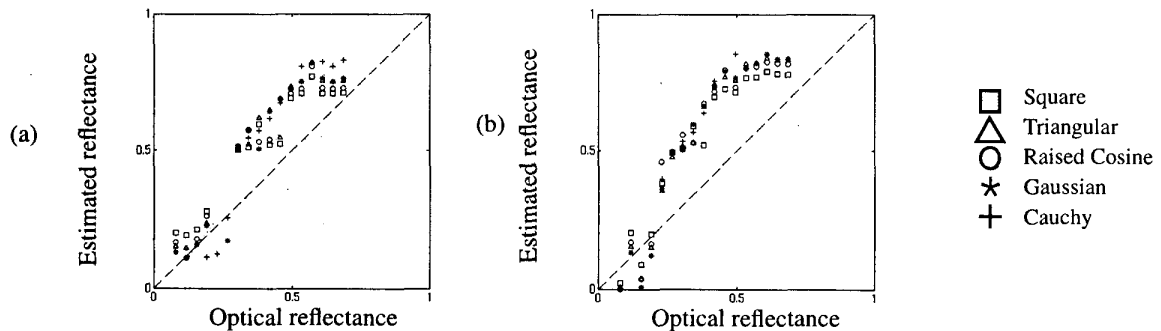
Figure 8: Comparison of estimated reflectance threshold (1-Θ) from sector merge width versus optical reflectance associated with scanning threshold. Kodak test chart on (a) HP scanner, (b) Apple scanner.

Table 1: PSF width estimation summary using Kodak star

PSF	HP Scanner			Apple Scanner		
	Mean Width Parameter Estimate	Standard Deviation	Benchmark Width Estimates	Mean Width Parameter Estimate	Standard Deviation	Benchmark Width Estimates
Square Pulse (w_S)	3.71	1.95	2.67 - 3.39	2.81	2.23	2.39 - 3.32
Triangular Pulse (w_T)	3.75	1.08	4.22 - 5.26	3.11	1.90	3.56 - 5.65
Raised Cosine (w_C)	4.46	1.39	4.57 - 5.65	3.88	1.88	3.53 - 4.51
Gaussian (σ)	1.06	0.51	0.90 - 1.14	0.61	0.29	0.77 - 1.22
Cauchy (α)	0.79	0.31	0.50 - 0.65	0.57	0.28	0.46 - 0.74

Table 2: PSF width estimation comparing original and corrected T2 star configuration on HP scanner

PSF	Mean Width Parameter Estimate (without) with correction	Standard Deviation (without) with correction	Knife Edge Width Estimates
Square Pulse (w_S)	(4.51) 3.14	(2.49) 1.25	2.67 - 3.39
Triangular Pulse (w_T)	(4.91) 3.91	(2.12) 1.30	4.22 - 5.26
Raised Cosine (w_C)	(5.48) 4.21	(2.15) 1.19	4.57 - 5.65
Gaussian (σ)	(1.01) 0.89	(0.46) 0.33	0.90 - 1.14
Cauchy (α)	(0.79) 0.76	(0.31) 0.37	0.50 - 0.65

the reflectances of the paper and ink not being 1 and 0.

The accuracy of the w and Θ estimates depends on both the δ_c and the τ_1 values. Estimates of τ_1 are more influenced by the star target than are δ_c values. A couple of white pixels remaining in the trajectories due to the anisotropic PSF prevents total black from being achieved and distorts the estimate of τ_1. The quality of the numerical estimate of the AED functions is another factor affecting the quality of the results of PSF width and threshold estimation.

6. Summary

This paper expands on the method of using a star target to estimate the displacement of an edge, δ_c. Edge spread will not provide estimates of the individual parameters w and Θ from the scanner model. By taking the edge shift quantity, δ_c, and combining it with the sector merge width, τ_1, the scanner parameters can be estimated individually. However, estimation of w requires an assumption of the PSF shape. A false assumption of PSF shape will introduce a bias in the parameter estimates.

The estimation is based on the measurements of the edge displacement in regions of the pattern where there is no aliasing, and measurements of the interference effect between two or more close edges. These two categories of measurements together provide the information necessary to estimate the two parameters: PSF width and binarization threshold. Corrections for non-ideal star charts that could be used in the future for multiple defects, such as printing and photocopying were also provided.

7. Acknowledgement

8. References

[1] H. S. Baird, "Calibration of document image defect models," Proc. of Second Annual Symposium on Document Analysis and Information Retrieval, Las Vegas, Nevada, Apr. 1993, pp. 1-16.

[2] H. S. Baird and G. Nagy, "A self-correcting 100-font classifier", in Document Recognition, L. Vincent and T. Pavlidis, editors, Proc. SPIE Vol. 2181, pp. 106–115, 1994.

[3] E. H. Barney Smith, "Characterization of Image Degradation Caused by Scanning," Pattern Recognition Letters, Vol. 19, No. 13, 1998, pp. 1191-1197.

[4] E. H. Barney Smith, "Optical Scanner Characterization methods Using Bilevel Scans," Ph.D. Thesis, Rensselaer Polytechnic Institute, Dec. 1998.

[5] T. K. Ho and H. S. Baird, "Large-Scale Simulation Studies in Image Pattern Recognition," IEEE Trans. on Pattern Analysis and Machine Intelligence, Vol. 19, No. 10, Oct. 1997, pp. 1067-1079.

[6] T. Pavlidis, M. Chen, and E. Joseph, "Sampling and Quantization of Bilevel Signals," Pattern Recognition Letters, Vol. 14, Jul. 1993, pp. 559-562.

[7] P. Sarkar, G. Nagy, J. Zhou, D. Lopresti, "Spatial Sampling of Printed Patterns," IEEE Trans. on Pattern Analysis and Machine Intelligence, Vol. 20, No. 3, Mar. 1998, pp. 344-351.